Spatial Confinement Effects of Laser Produced Plasmas in Air and under Water

Yan Qiu[1], Zhi Zhang[1], Jian Wu[1], Han Yu[1], Huantong Shi[1], Xingwen Li[1], Qian Wang[2]

1 State Key Laboratory of Electrical Insulation and Power Equipment, Xi'an Jiaotong University, Shaanxi 710049, China

2 School of Sciences, Xi'an University of Technology, Shaanxi 710048, China

Abstract: The evolution of laser produced plasmas with spatial confinement is very different from its evolution in free space in terms of dynamics and radiation, which is likely with potential application values. It's important to understand the physical processes of laser-produced plasma and pulse laser ablation in liquids in this state. This paper presented diagnostic results of plasma evolution both in air and water under spatial constraints.

Keywords: spatial confinement; shock wave; bubble splitting

1. Introduction

Since the spatial confinement effects in the air that can help to enhance plasma radiation was reported, it has been recognized that this is a simple and reliable way to improve the LIBS signal by introducing mechanical structures instead of any energy sources. Although more and more space-constrained structures have been designed (such as cylinder, plate wall, hemisphere, groove, and even cone) [1-2], the mechanism for improving plasma spectroscopy in air is still needed to be experimentally verified. In addition, when the plasma evolves with spatial confinement under water, the enhancement of the spectral radiation would disappear. In this case, the plasma evolution undergoes more complex material breakdown processes [3].

Under the effects of spatial constraints, the dynamic evolution process of plasma becomes more complicated (especially underwater plasma evolution). Therefore, it is necessary to apply plasma diagnostic methods to study the evolution of space-constrained plasma both in air and under water. In this paper, the evolution of plasma self-luminous and its shock waves has been studied using fast imaging and picosecond laser probing. While the dynamics of the plasmas and shock waves could be visualized, the radiation evolution could be presented simultaneously. The bubble evolution induced by plasma under water could be also obtained by picosecond laser shadow.

2. Experimental Setup

The schematic diagram of the experimental setup is shown in Fig.1. The laser ablation process was performed using a Q-switched Nd:YAG pulse laser source (SGR-60, <3 J, Beamtech Optronics Co., Ltd.) with 1064 nm wavelength, 8ns full width at half maximum (FWHM). A plano-convex (L1) with a focal length of 32 mm in the air was placed in a glass container filled with pure deionized water, of which the focal length is approximately four times that of the original in water. The laser passed through the glass wall of the container and then was focused on the surface of the aluminum target which was fixed on a sample holder under water, as shown in the inset of Fig. 1. A pair of parallel aluminum plate walls (W) was used to confine the produced plasma, shock waves and bubbles. The sample holder with the target was connected to a three-axis stage and we made the focus of the laser beam in the middle of the two walls by adjusting its displacement in the *z* direction. Time-resolved laser shadowgraphy was performed to track the shock waves and bubbles. The shadowgraphy was imaged to a CCD camera (Canon, 700D) coupled with a picosecond laser beams (532nm), and a '4-*f*' optical imaging system (L2-L3) was used for imaging the probe beams to the CCDs with the focal length 250 mm.

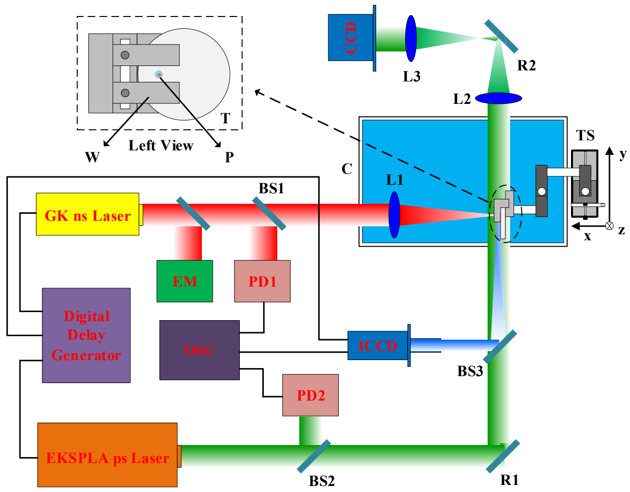

L: lens; BS: beam splitter; R: reflector; T: target; P: plasma; C:container
EM: energy meter; PD: photon detector; OSC: oscilloscope; TS: three-axis stage

Fig. 1. Schematic diagram of the experimental setup.

An ICCD camera (Andor istar DH734) was located laterally to the sample surface, utilized to detect the plasma self-emission. The timing of the Nd:YAG laser, probe laser, and ICCD was controlled by digital delay pulse generator (DG535, Stanford Research Systems). The delay could be set so small that we could observe the evolution of shock waves and bubbles through the time-resolved shadowgraphy. Both the time gate delay from the laser purse and gate width can be determined from the signal of ICCD gate monitor. In addition, a high-speed visible photon detector (DET10A, Thorlab) was used to monitor the action of laser and record the time stamp.

3. Spatial Confinement in Air

The nanosecond laser-produced plasma was investigated using time-resolved spectroscopy, fast imaging, interferometry. As comparison, a pair of plate walls was placed at both ends of the target in a suitable distance to constrain plasma evolution. Experimental results confirmed that the plasma was constricted by the reflected shock associated with a temperature and density gradient. [4]

The temporally resolved spectral emission was recorded, as shown in Fig. 2. The enhancement of plasma emission can be easily distinguished, with a maximum enhancement factor up to ~ 5.2. For further studying the differences on plasma evolution, space-time resolved plasma self-luminous image with and without confinement, obtained by ICCD camera are given in Fig. 3. It appears that when the plasma at the center of the constraint was compressed, the plasma morphology approached the rectangular form, accompanying significant plasma radiation enhancement. The change in plasma shape should be related to the enhancement of radiation.

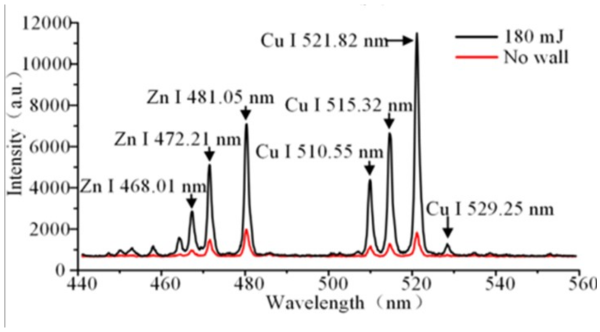

Fig. 2. The temporally resolved spectra of plasma produced by 180 mJ laser with (black) and without (red) confinement. The wall distance is 9 mm.

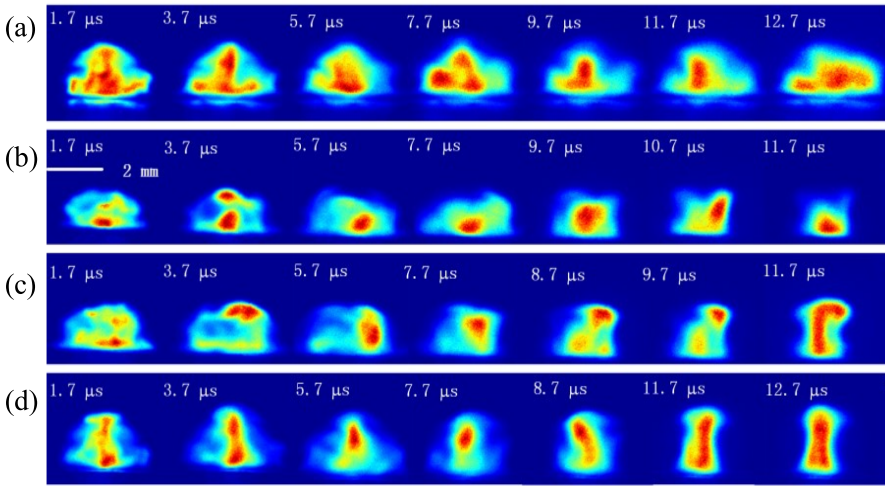

Fig. 3. Temporally resolved plasma self-emission images without (a) and with confinement. The wall distance is 9 mm, and the laser energy is 140 mJ(b), 160mJ(c), 180mJ(d).

In addition, with the method of laser interference, the internal structure of the plasma could be clearly presented. The fringe shift profiles were obtained using fringe trace method, as shown in Fig. 4. The rapid expansion of the shock waves, as well as the reflection and reverse motion of the shock waves caused by the plate walls in the later stage could be clearly observed. Before the delay time of 5.7 μs in Fig. 3, the reflective shock wave fronts are clear. After that, the reflective shock wave fronts which are approaching the plasma center become less distinct; this is because the density of the plasma is low and the gradient of the density is small. From the fringe shift profiles, the electron density could be deduced, which indicated that at 5.7 μs, the density of the air near the Al-plates was enhanced although the plasma was not influenced, revealing the reflection of the shock waves occurred at this moment. After that, the plasma began to be compressed until the reflective shocks collided at the middle.

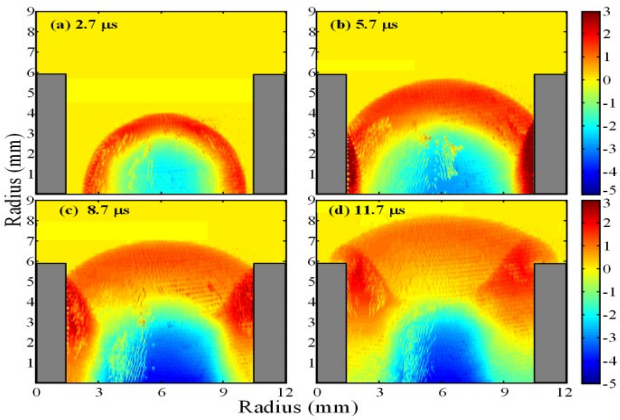

Fig. 4. Fringe shift profiles extracted from the raw interferograms. Time delay (a) 2.7μs, (b) 5.7μs, (c) 8.7 μs, (d) 11.7 μs.

By comparing the analysis results of Fig. 4 with the fringe shift analysis of free evolution, the plasma had a larger negative fringe shift in the central region of the plasma plume when it received compression by the reflected shock waves. This showed that under the effects of spatial constraints, the electron density in the plasma plume was significantly improved, which would become an important cause of spectral radiation enhancement.

4. Spatial Confinement under Water

The detailed process after ablation laser irradiation was shown by Fig. 5. Images in Fig. 5(a) were captured in no space confinement condition. The red lines in the two figures indicate the position of the aluminum target surface. Firstly, we could see that shock waves caused by the laser-induced plasma emerges, and then it expands as a hemisphere. There were several lines parallel to the target surface and numerous circles. The lines parallel to the target surface were the reflection waves of the plasma shockwave from the target. And the small circles were due to laser pulse ablation of nanoparticles in pure deionized water with a few nanoparticles which were produced when we focused repeatedly on the target to take images at different delays. From the figure we could see that the bubble started to appear at this moment of 4.88μs, and it expanded in a hemispherical shape until 186μs when the bubble reached the maximum radius [5]. After that, since the pressure inside the bubble started to be smaller than the external pressure, the bubble began to shrink down until 403μs. At the end of bubble shrinkage shown by image at 406μs, the bubble collapsed and generated a shock wave, releasing energy outward. At the time of 427μs, we could observe the second cavitation bubble generated, and then began to expand but not as a standard hemisphere shape.

The images in Fig. 5(b) are in a constrained condition with the wall distance at 4 mm. We can observe that the early shock waves repeatedly oscillated in the parallel aluminum plate walls and then propagated beyond the constraints as the images shown at 2.92μs and 5.20μs. The shock waves and reflected wave were more intense than in unconstrained conditions, which caused the water between the walls to oscillate violently. There were obvious differences between the process of the first bubble oscillation in a constrained condition with the wall distance at 4 mm and that in no space confinement condition. On one hand, the first bubble appeared at the time about ~ 20μs, which was significantly later than the unconstrained contrast experiment at the time of 4.88μs. On the other hand, the collapse time of the first bubble was also later than that in the case of no space confinement condition, which was 486μs in the former and 406μs in the latter.

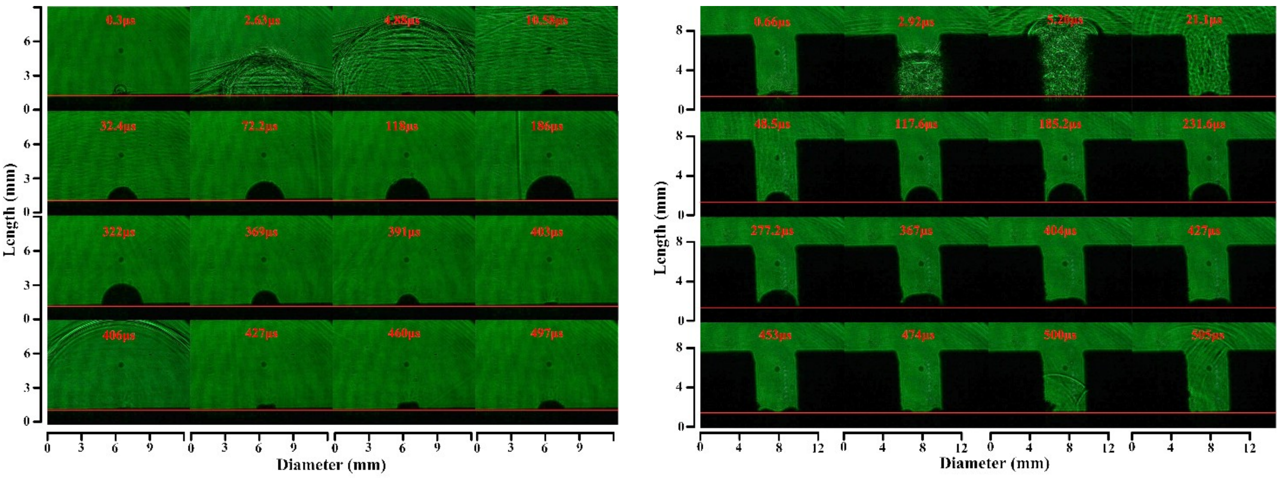

(a) (b)

Fig. 5. Evolution of shock waves and bubbles in laser ablation in liquids. (a) The images captured in no space confinement condition. (b) The images captured in a constrained condition with the wall distance at 4 mm.

In the experimental results of laser ablation in liquid in a space confinement condition, we observed an interesting phenomenon, which had not been well observed in the previous literature. As shown in Fig. 5(b), although the evolution behavior of the first period bubbles in the expansion process was similar to that in an unconstrained condition, the shrinkage process was completely different from that in an unconstrained condition. In the process of the shrinkage of the first bubble, due to the constraint of the walls, the bubble front fell rapidly and the bubble began to evolve like a flat from a hemispherical. Eventually, the center of the bubble collapsed before the edge of the bubble, splitting into left and right small bubbles that continued to shrink down. Based on the subsequent repeated experiments, we observed that a weak shock wave released by the contact propagated outward when the center of the bubble touched the target surface in this process. After the collapse of the left and right bubbles, two new shock waves were generated with the lower left corner and the lower right corner as the center of the circle at which time energy was released respectively shown by images at 500μs, and 505μs. Due to the stability and repeatability problems of laser ablation in liquids, the two small bubbles separated by different repeated pulses had different volumes, different collapse time and different shock waves. We speculated that the reason for this special phenomenon was that the interaction between the two walls on the bubble edge led to the bubble center shrinking faster than the bubble edge during the bubble contraction process, resulting in the formation of left and right small bubbles. More research is needed to elucidate this phenomenon.

Besides the shadowgraphy method, we also obtained the detailed date about the plasma induced in laser ablation in liquids in order to explore the effect of space constraint on plasma. Fig. 6 showed the sequence of temporally resolved plasma self-emission images taken by ICCD with the width of 10 ns and the accumulative number of 10. Images in Fig. 6(a) were captured in no space confinement condition while images in Fig. 6(b) were in a constrained condition with the wall distance at 4 mm. It was found that the plasma lifetime under space constraint was shorter than that without space constraint and the plasma self-emission intensity in the former was lower than that in the latter under the same time delay. This indicated that the spatial confinement attenuated rather than enhanced the plasma generated by laser ablation in liquids. The reason might be that when we performed pulse laser ablation in liquids in the case of spatial confinement condition, the generated nanoparticles were concentrated between the two walls and difficult to diffuse, compared with the unconstrained condition. As a result, some of the laser energy would be used to ablate the nanoparticles when the next laser pulse arrived, so there would be less laser energy reaching the surface of the target leading to the weaker plasma self-emission intensity. In addition, the liquids were easier to break down when the interparticle distance between nanoparticles was small from the research of Mark-Robert Kalus [6].

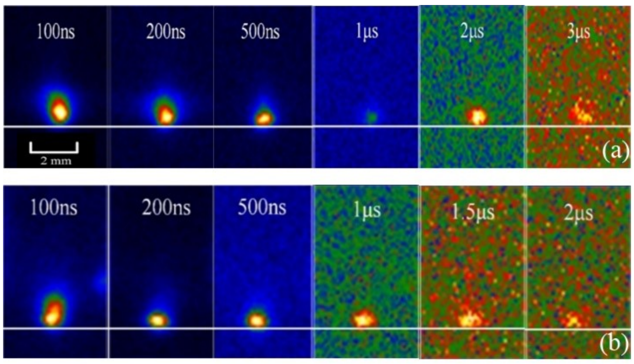

Fig. 6. The sequence of temporally resolved plasma self-emission images. (a) The images captured in no space confinement condition. (b) The images captured in a constrained condition with the wall distance at 4 mm.

Therefore, we couldn't rule out the situation that the ablation laser broke down the liquid to produce water plasma when the previously generated nanoparticles were concentrated in the space constraint region, which also reduced the amount of laser energy reaching the target surface. From Fig. 6(b), we noted that the initial plasma shown by images at 100 ns looked more like a rod compared to the same time in unconstrained conditions. This further confirmed our hypothesis that this might be due to laser ablation of previously generated nanoparticles in the vertical target surface path to form plasma or breakdown of liquids to produce water plasma.

5. Conclusion

In this paper, the evolution of plasma self-luminous and its shock waves has been studied using plasma diagnostic methods with confinement both in air and under water.

Experiments of plasma under in air under the effects of spatial constraints show the plasmas will be compressed by the reflected shocks, formed by the obstruction of a pair of plate walls, which induces the increases of plasmas density, resulting in the enhancement of spectral intensity. The enhancement factor is about 5.2. We found a new phenomenon in the experiment of laser ablation in liquids in a space confinement condition. In the process of the shrinkage of the first bubble, due to the constraint of the walls, the bubble center shrinks faster than the bubble edge and collapses before the edge of the bubble, splitting into left and right small bubbles that continue to shrink down. In addition, the spatial confinement attenuates rather than enhances the water plasma generated by laser ablation in liquids, which may be due to laser ablation of previously generated nanoparticles or the breakdown of liquids to produce water plasma.

6. References

[1] Shen X K, He X N, Huang H and Lu Y F, Applied Physics Letters, **91**, 30 (2007).
[2] Zhe W, Zongyu H, Siu-Lung L, et al., Optics Express, **20** Suppl 6 (2012).
[3] Chen J, Li X, Gu Y, et al. Journal of colloid and interface science, **489**, (2017).
[4] Li X , Yang Z , Wu J, et al., Journal of Physics D: Applied Physics, **50**, 1 (2017).
[5] Lam J , Lombard J , Dujardin C , et al., Applied Physics Letters, **108**, 7 (2016).
[6] Kalus M R, Reimer V, Barcikowski S, et al., Applied Surface Science, **465**, (2019).